Phosphorylation Regulates the ADP-Induced Rotation of the Light Chain Domain of Smooth Muscle Myosin†

Jeremy Gollub,‡ Christine R. Cremo,§ and Roger Cooke*,||

Graduate Group in Biophysics, Department of Biochemistry and Biophysics, and Cardiovascular Research Institute, University of California, San Francisco, California 94143-0448, and Department of Biochemistry and Biophysics, Washington State University, Pullman, Washington 99164-4660

Received February 4, 1999; Revised Manuscript Received May 28, 1999

ABSTRACT: We have observed the effects of MgADP and thiophosphorylation on the conformational state of the light chain domain of myosin in skinned smooth muscle. Electron paramagnetic resonance (EPR) spectroscopy was used to monitor the orientation of spin probes attached to the myosin regulatory light chain (RLC). Two spectral states were seen, termed here "intermediate" and "final", that are distinguished by a ∼24° axial rotation of spin probes attached to the RLC. The two observed conformations are similar to those found previously for smooth muscle myosin S1; the final state corresponds to the major conformation of S1 in the absence of ADP, while the intermediate state corresponds to the conformation of S1 with ADP bound. Light chain domain orientation was observed as a function of the MgADP concentration and the extent of RLC thiophosphorylation. In rigor (no MgADP), LC domains were distributed equally between the intermediate state and the final state; upon addition of saturating (3.5 mM) MgADP, about one-third of the LC domains in the final state rotated ∼20° axially to the intermediate state. The progression of the change in populations was fit to a simple binding equation, yielding an apparent dissociation constant of ∼110 μM for skinned smooth muscle fibers and ∼730 μM for thiophosphorylated, skinned smooth muscle fibers. These observations suggest a model that explains the behavior of "latch bridges" in smooth muscle.

Smooth muscle's ability to maintain high force at a low energy cost presents an important biological puzzle. Smooth muscle is markedly more economical than skeletal muscle in maintaining tension during a long contraction. Smooth and skeletal muscles differ in both biochemical and structural aspects, and these differences may be directly related to differences in their economy of tension maintenance (for a discussion, see ref *1*).

One important difference between smooth and skeletal muscles concerns the effect of phosphorylation of the myosin regulatory light chain (RLC).[1] RLC phosphorylation may play several roles in smooth muscle. The activity of the force-generating protein (myosin) is upregulated in smooth muscle by phosphorylation of serine 19 of the RLC (*2*−*8*). Although the analogous site can be phosphorylated in skeletal muscle, the consequences to regulation are minor (*9*). Initially upon activation, smooth muscle myosin generates increasing force up to a maximum; the velocity of contraction and ATPase activity increase along with tension. If activity is maintained, however, force remains high while velocity and ATPase decline markedly over several minutes (*9*−*12*). The extent of phosphorylation of the RLC has been observed to increase and then decrease along with ATPase level (*10*, *11*). This so-called "latch" state is more pronounced in "tonic", e.g., some arterial, than in "phasic", e.g., intestinal, smooth muscle types (*1*, *13*−*15*). The latch state, which is highly economical at maintaining tension, is likely involved in various biological functions such as vasoconstriction in response to cold. While a similar time course of ATPase activity exists for long tetanic contractions in skeletal muscle, the decrease in activity is less than in smooth, and it is not accompanied by a decrease in the extent of RLC phosphorylation.

The change in economy, from low economy early in contraction to high economy late in contraction, is attributed to the progressive creation of "latch bridges". It is thought that these are dephosphorylated myosin heads that interact with actin, generating force but cycling much more slowly than active, phosphorylated heads (*10*, *15*−*18*). An important question is why a dephosphorylated myosin head would cycle more slowly, and thus apply force to the actin filament more economically, than a phosphorylated, active myosin head.

A candidate for a molecular basis for the latch state was seen in a conformational change in smooth myosin S1 (a single myosin head) bound to actin. The myosin head consists of a large, globular catalytic domain and a narrower, more extended light chain domain (LC domain). The catalytic domain consists of a single protein heavy chain, and contains

† This work was funded by grants from the U.S. Public Health Service: AR42895 (R.C.) and AR40917 (C.R.C.). J.G. is a predoctoral fellow of the American Heart Association.

‡ Graduate Group in Biophysics, University of California.

§ Department of Biochemistry and Biophysics, Washington State University.

|| Department of Biochemistry and Biophysics and Cardiovascular Research Institute, University of California.

[1] Abbreviations: EPR, electron paramagnetic resonance; ϵATP, 1,N^6-ethenoadenosine 5′-triphosphate; IASL, 4-(2-iodoacetamido)-2,2,6,6-tetramethyl-1-piperidinyloxy (spin-label); RLC, myosin regulatory light chain; S1, myosin subfragment 1; SL-ADP, 3′-deoxy-2′-(2,2,5,5-tetramethylpyrrolidine-1-oxyl-3-carboxylate) adenosine 5′-diphosphate.

10.1021/bi990267e CCC: $18.00
Published on Web 07/10/1999

the actin and nucleotide binding sites (*19*). The LC domain contains two light chains and probably acts as a lever arm in force generation, rotating axially to amplify a conformational change in the globular catalytic domain (the "power stroke"; for a review, see ref *20*). Cryoelectron microscopy revealed an axial rotation of the LC domain upon MgADP release, toward the "barbed" end of the actin filament, of 23° in smooth muscle S1 (*21*) and 32° in a nonmuscle myosin (*22*). This rotation was in the direction expected for the power stroke. Our previous work (*23*) in which we employed a spin probe on the RLC of S1 showed that this rotation occurred in smooth, but not skeletal, S1, with an apparent dissociation constant for MgADP of ~5 μM. The LC domains of both smooth and skeletal S1 occupied very similar positions with MgADP bound, a state that would presumably represent the end of the power stroke for skeletal myosin (*20*). Upon the release of MgADP, the smooth LC domain rotated ~24°; no such rotation was observed in skeletal myosin.

The data described above, along with models derived from the crystal structures of skeletal and smooth muscle S1, suggest that the light chain domain can adopt at least three orientations relative to the catalytic domain. Recent spectroscopic observations of invertebrate muscle revealed two distinct conformations of the LC domain, distinguished by an axial angle of at least 36°, which varied in population according to the physiological state of the muscle and were interpreted as pre- and post-power stroke states (*24*). Additionally, the crystal structure of smooth muscle S1 showed the LC domain rotated relative to the catalytic domain by ~70° compared to the orientation observed previously for skeletal S1 (*19*, *25*). This structure may represent the beginning of the power stroke, and we characterize it as the "initial" position of the LC domain. The position of the LC domain observed by Rayment et al. in the crystal structure of skeletal S1 (*19*) appears to be similar to the orientation observed by electron microscopy of smooth muscle S1 in the presence of ADP by Whittaker et al. (*21*). Following the above nomenclature, we call this an "intermediate" position, representing the end of the power stroke in skeletal muscle. As noted, the smooth muscle myosin S1 LC domain continues to rotate along the same general path upon the release of ADP into the "final" position, observed by Whittaker et al. (*21*).

We report here on experiments that strengthen the hypothesis that the isomerization of smooth muscle myosin from the intermediate state to the final state may be important to the latch phenomenon. As described previously (*23*, *26*), we have used electron paramagnetic resonance (EPR) spectroscopy to monitor the orientation of the smooth muscle myosin LC domain with a nitroxide probe placed on the RLC. EPR spectroscopy provides a powerful tool for determining the orientation of a spin probe in oriented systems such as muscle fibers (*27*−*29*).

This study extends the approach to labeled, skinned gizzard muscle prepared by exchanging labeled RLC for the endogenous RLC in the muscle. In our previous studies, skeletal fibers were decorated with labeled smooth S1. We find the same two states, or orientations of the LC domain, in the labeled gizzard muscle as in our previous experiments with labeled S1. However, the populations of the two states are different, with both states populated in either the presence or absence of MgADP (rigor). The distribution between the states is altered by addition of MgADP, but the apparent affinity of MgADP is lower than that observed for S1. The effect of thiophosphorylation of the myosin RLC is a further weakening of the ability of MgADP to effect the conversion between the two states. We propose a simple model to explain these results which has the potential to explain the behavior of latch bridges.

MATERIALS AND METHODS

Solutions. The exchange solution consisted of 50 mM KCl, 50 mM TES (pH 7.0), and 10 mM EDTA. The rigor solution consisted of 120 mM KCl, 5 mM $MgCl_2$, 20 mM TES (pH 7.0), and 1 mM EGTA. The ADP solution consisted of rigor solution with 10 mM glucose, 1 mg/mL hexokinase (Sigma, St. Louis, MO), 250 μM diadenosine 5′-pentaphosphate (AP_5A, Sigma), and variable ADP concentrations. The concentration of MgADP was calculated assuming that the binding constant of ADP for Mg is equal to 1470 M^{-1}. The maximum MgADP concentration was 3.5 mM (5 mM ADP) in dephosphorylated samples and 16.6 mM (20 mM ADP, total Mg^{2+} concentration increased to 20 mM) in thiophosphorylated samples.

Protein Purification. Myosin was purified (*30*) from frozen chicken gizzards (Pell-Freeze, Rogers, AR). RLC was isolated from purified smooth muscle myosin (*31*), lyophilized, and stored at −80 °C. Myosin light chain kinase (MLCK) was prepared as previously described (*32*).

Labeling RLC. The sulfhydryl group of Cys-108 of chicken gizzard RLC was labeled with the paramagnetic probe, 4-(2-iodoacetamido)-2,2,6,6-tetramethyl-1-piperidinyloxy (IASL) (Aldrich, Milwaukee, WI). The RLC was incubated in rigor solution with 10 mM DL-dithiothreitol (DTT) and 5 M guanidine hydrochloride for 8−12 h at 0 °C to reduce disulfide bonds. DTT and guanidine hydrochloride were removed by dialysis for 4 h at 0 °C with rigor solution containing 0.1 mM tris(2-carboxyethyl)phosphine hydrochloride (TCEP) (Molecular Probes, Eugene, OR), followed by gel filtration into rigor solution, after which 1 mM IASL was added. After labeling for 3−12 h at 0 °C, free IASL was removed by extensive dialysis into exchange solution.

Preparation of Muscle Sections. Gizzards, flash-frozen in liquid N_2 (Pell Freeze), were trimmed and partially thawed. Thin sections were dissected perpendicular to the tough internal epithelium and to the long axis of the organ, across sheets of circular muscle fibers, such that "pseudo-fibers" composed of muscle cells joined by connective tissue ran parallel to the plane of the section. Sections were chemically skinned by shaking at 4 °C for 12−16 h in a rigor solution with a final concentration of 50% (v/v) glycerol, 5 mM DTT, and leupeptin, pepstatin A, and trypsin inhibitor (0.05 mg/mL each) (Boeringher Mannheim, Indianapolis, IN). Fresh gizzards were treated similarly within 1 h of killing, but never frozen. All sections were stored in fresh skinning solution at −20 °C.

Exchange of Labeled RLC for Native RLC. Muscle sections were incubated in exchange buffer containing 1−2 mg/mL labeled RLC for 2 h at 0 °C while being shaken. The solution was heated to 42 °C for 30 min, after which TES was added to a concentration of 100 mM (2 M stock, pH 7.0) and $MgCl_2$ to 12 mM (final pH of 6.6). The mixture was incubated at 0 °C for 15 min, and the muscle sections

were then removed and placed into rigor solution. It has been previously shown that similar exchange procedures do not alter the phosphorylation-dependent regulation of isolated smooth muscle myosin (*31*, *33*−*35*). The extent of exchange varied by preparation, and was estimated from isoelectric focusing gel electrophoresis. The depletion of unlabeled, native RLC indicated that from 50 to 90% of the myosin heads were exchanged, while the presence of excess labeled RLC indicated that the total labeled RLC content of the muscle sections exceeded the total exchanged myosin head content by 20−50%.

Thiophosphorylation of Muscle Sections. Prior to exchange of RLC, muscle sections were incubated for 90 min at room temperature in solution containing 50 mM KCl, 50 mM TES (pH 7.2), 2 mM $CaCl_2$, 2 mM $MgCl_2$, 2 mM ATPγS, 5 μg/mL calmodulin (Sigma), and 20 μg/mL MLCK. Labeled RLC was incubated for 90 min at room temperature in solution containing 50 mM NH_4HCO_3 (pH 7.8), 0.1 mM EDTA, 0.1 mM EGTA, 2 mM $MgCl_2$, 2 mM $CaCl_2$, 5 μg/mL calmodulin, 20 μg/mL MLCK, and 2 mM ATPγS. The level of thiophosphorylation was checked by isoelectric focusing gel electrophoresis (pH 4−6). Exchanged samples with >90% thiophosphorylated RLCs were used for EPR experiments. Prior to thiophosphorylation, samples exhibited phosphorylation levels of <10%.

Fluorescence Spectroscopy. Gizzard sections were incubated in rigor solution containing 400 mM acrylamide and placed at the focus of a Nikon Diaphot 200 epifluorescence microscope, and baseline fluorescence levels were recorded (excitation at 320 nm and emission at 410 nm). 1,N^6-Ethenoadenosine 5′-triphosphate (25 μM) (ϵATP, Sigma) was added to the solution, and fluorescence levels were recorded. The sample was then washed with rigor solution containing 400 mM acrylamide, and fluorescence levels were recorded at 30 s intervals until fluorescence reached a minimum.

EPR Spectroscopy. EPR measurements were taken with an ER/200D EPR spectrometer from Bruker, Inc. (Billerica, MA). X-Band, first-derivative absorption spectra were obtained with the following settings: microwave power, 25 mW; center field, 3460 G; time constant, 500 ms; sweep time, 50 s; modulation, 2 G at a frequency of 100 kHz; and total sweep width, 125 G. Labeled smooth muscle sections mounted on a flat cell were located in the center of a TM cavity. Each spectrum used in data analysis represented the average of 10−40 distinct sweeps over a single experimental preparation. Spectra were recorded at room temperature, 18−22 °C.

The following protocol was carried out on each set of fibers or sections. Spectra of samples with the myosin filament/"pseudo fiber" axis aligned parallel to the magnetic field were first obtained for the rigor condition (muscle sections washed with exchange solution for 2 h to remove all nucleotide); the sample was then rotated 90° to obtain a spectrum with the sample axis perpendicular to the magnetic field. The sample was then incubated in 1−3 mL of ADP solution with the desired MgADP or Mg·ϵADP concentration for 20 min at 0 °C, and replaced on the flat cell. Spectra were obtained at each concentration with the sample axis parallel to the magnetic field. At the highest concentration that was used (usually 3.5 mM; 16.6 mM for thiophosphorylated samples), the cell was again rotated to obtain a spectrum with the sample axis perpendicular to the magnetic field. Fibers were returned to a nucleotide-free state by washing extensively (≥2 h) with exchange solution, with rigor solution containing 30 units/mL myokinase (Sigma), or with rigor solution adjusted to pH 6.6 containing 50 units/ml apyrase (Sigma) with a ∼3:2 ratio of ATPase:ADPase activity, and a spectrum was obtained with the sample axis parallel to the magnetic field and compared to the initial spectrum. Spectra were acquired over the course of 10−25 min at each MgADP concentration, except for the first and last spectra, which were collected for 20−40 min to reduce noise. Finally, the samples were either removed from the cell or washed with 10 mM ascorbate, which reduced all the spins, and a baseline spectrum was recorded. The baseline was subtracted from each spectrum, if substantially nonlevel. Spectra were compared with a spectrum of peroxylamine disulfonate (PADS) in solution to determine the magnetic field range and center. Peak positions and baseline crossings were determined relative to the PADS baseline crossings. The PADS splitting was taken to be 13.091 G and the center peak to correspond to a g value of 2.0056.

Spectra of unlabeled gizzard sections and rabbit semimembranosus fibers containing 3′-deoxy-2′-(2,2,5,5-tetramethylpyrrolidine-1-oxyl-3-carboxylate) adenosine 5′-diphosphate (SL-ADP), a spin-labeled ADP (*36*), were recorded similarly, except data collection times were shorter (5−10 min), and SL-ADP was not washed out afterward.

RESULTS

Orientation of Myofilaments. The experiments described below rely on an ordered array of myosin heads for interpretable data. Our previous work utilized the highly ordered array of actin filaments in skeletal muscle to order exogenous smooth muscle myosin heads (S1). The myofilaments of smooth muscle are generally not as well ordered as in skeletal muscle. It was therefore necessary to establish that the myosin heads in our samples were ordered in a manner comparable to those in skeletal muscle.

The orientation of myosin heads, attached to actin, in skinned sections of gizzard muscle was observed using a spin-labeled ADP analogue (SL-ADP). This compound binds to myosin in skeletal muscles in an oriented fashion (*36*). Thin sections of smooth muscle tissue were incubated in 25 μM SL-ADP in rigor solution, aligned such that "pseudofibers" were parallel or perpendicular to the applied magnetic field, and EPR spectra were recorded (Figure 1A). The resultant spectra consisted of three large peaks arising from free SL-ADP, and smaller peaks arising from bound nucleotide (see the Figure 1 labels and caption). Spectra obtained with the fiber axis parallel to the magnetic field differed significantly from those obtained with the perpendicular orientation, an indication of ordered myosin heads.

The spectrum arising from gizzard sections was similar to that arising from highly ordered semimembranosus (skeletal) fibers (Figure 1B). This similarity indicates that the myofilaments in gizzard muscle are generally parallel to the fiber axis created by slicing across the circular muscle sheets as described in Materials and Methods. The degree of order of myosin heads in the two preparations can be estimated from the spectra of the bound probes (*27*). The average probe angle was determined from the splitting between the low-field peak and high-field trough of the

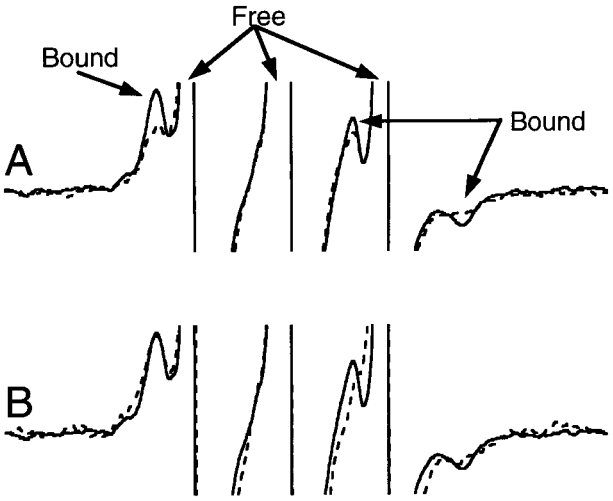

FIGURE 1: First-derivative, X-band absorption EPR spectra of samples containing SL-ADP. (A) SL-ADP (25 μM) in gizzard sections: (—) sample parallel to the magnetic field and (- - -) sample perpendicular to magnetic field. There are two populations of SL-ADP, free and bound to myosin. Each population produces three lines in the spectrum. The free SL-ADP produces sharp lines, labeled "free" in the figure, truncated in the figure. The bound SL-ADP produces smaller, more spread-out features, labeled "bound". The central line of each overlaps. The difference between spectra of parallel and perpendicular samples represents ordered probes. (B) (—) SL-ADP (25 μM) in gizzard sections and (- - -) SL-ADP (25 μM) in rabbit semimembranosus (skeletal) fibers. The spectra are similar, indicating that myosin heads bound to actin in gizzard muscle cells are ordered in a manner similar to that of myosin heads in skeletal fibers. Spectra were recorded with a modulation of 2 G, a time constant of 500 ms, a center field of 3460 G, and a sweep width of 100 G.

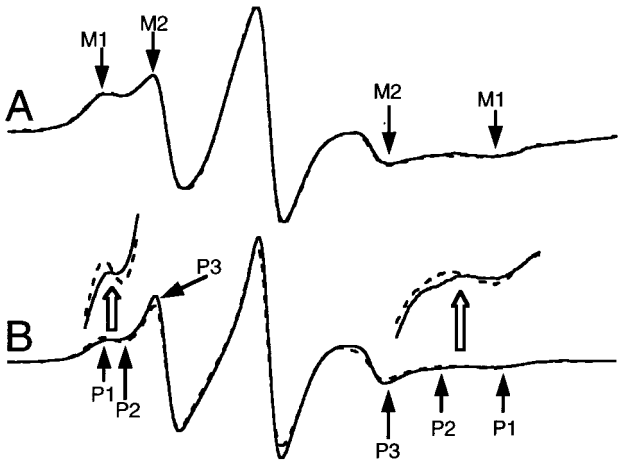

FIGURE 2: EPR spectra of labeled gizzard sections with (—) no nucleotide and (- - -) saturating MgADP. (A) Labeled gizzard sections, homogenized. There are two populations, labeled M1 and M2, representing spin probes with two distinct mobilities. Each gives rise to three lines; the central lines overlap. The two populations are of roughly equal intensity in this spectrum. (B) Labeled gizzard sections, aligned parallel to the magnetic field. The low- and high-field regions are vertically expanded (above the main spectrum) for clarity. There are three populations, labeled P1−P3; the central lines of each overlap. P2 especially is difficult to discern due to overlap with P3 in the low-field region, and with P1 in the high-field region. Upon addition of saturating MgADP, the intensity of P2 decreases and that of P1 increases, producing the differences seen here between spectra.

spectral component arising from bound probes. For gizzard, this splitting is ∼50.5 G, indicating a mean probe orientation of 50 ± 5° to the fiber axis; the orientation of the same probe in skeletal muscle has previously been determined to be 55 ± 5° (*36*). The width of the distribution of probes about the mean angle was determined from the ratio of the absolute heights of these two spectral features; in gizzard, the ratio of high- to low-field peak height is 0.33, indicating a width of 20 ± 6°, versus 16 ± 4° in skeletal muscle (*36*). The similarity of the probe orientation in gizzard and skeletal muscle indicates that the degree of order of myosin heads is similar in the two muscle types. The small differences that do exist may reflect differences in the active site structures of smooth and skeletal myosin or, possibly, a slightly less well ordered myofilament array in gizzard.

RLC Exchange into Muscle Sections. Chicken gizzard regulatory light chain labeled with IASL at Cys-108, as used previously in skeletal muscle (*26*) and smooth muscle myosin S1 (*23*), was exchanged for native light chain in gizzard muscle sections (see Materials and Methods). The characteristics of our probe in these preparations are similar to those ascertained for the same probe on skeletal muscle myosin and smooth muscle S1, as discussed below.

Probe Mobility. To determine the orientation of the LC domain, the spin probe employed must be well-ordered and substantially immobilized by the protein surface to which it is bound. Figure 2A shows the spectra of homogenized, isotropically oriented samples, which are sensitive to the mobility of the probe. A highly mobile probe population in these conditions gives rise to three sharp, narrowly separated peaks. As mobility decreases (probes tumble less quickly, or are more restricted in their motion), these peaks broaden and the splitting between them widens. A completely, or nearly, immobile probe population gives rise to a characteristic spectrum with a wide splitting (*37*).

Our probe gives rise to two spectral components, labeled M1 and M2 in Figure 2A, representing two populations with distinct mobility characteristics. Similar populations were seen in studies of S1 (*23*) where they were analyzed and discussed in more detail. M1 has a low-field peak to high-field trough splitting of 64 G, representing a population of probes that is well-immobilized by the protein surface. Following the method of Griffith and Jost (*37*), we modeled this as rapid diffusion in a cone with a full width of ∼60°. While not ideal, this motion is sufficiently restricted that the probe reports on the orientation of the adjacent protein surface, in this case the LC domain. The second population, M2, has a splitting of 39 G. This is quite mobile, equivalent to rapid diffusion in a cone with a full width of ∼140°. This population does not usefully report on the protein orientation; our analysis will concentrate on M1 except to point out where the presence of M2 hinders analysis. The presence of two populations with different mobilities could indicate that probes are in equilibrium between strong and weak interaction with the protein surface, with slow exchange between states. However, individual preparations have different ratios of M1 to M2 (M2 ranges from ∼50% to ∼75% of the total signal; in Figure 2A, M2 is ∼50% of the total signal), while only probes giving rise to M1 change orientation observably upon binding of MgADP to myosin, as discussed below. We conclude that M2 arises at least in part from nonspecifically or improperly bound RLCs.

A change in the spectrum of an oriented sample can reflect an actual change in the orientation of the protein to which a

spin probe is bound, or it can indicate a change in the binding mode of the probe on the protein, with no gross change in protein conformation. The latter possibility is nearly certain to produce a change in probe mobility, since a reorientation of the probe relative to the protein or a change in the local protein surface with which it interacts will alter the constraints on probe rotation and diffusion. Addition of 5 mM ADP did not alter the spectrum of an isotropic sample in rigor solution (Figure 2a). This indicates that the mobility of the probes was not affected by the presence of MgADP. We therefore conclude, as in our previous work, that changes in the spectra of oriented samples due to addition of MgADP (discussed below) result from actual changes in protein orientation.

Probe Orientation and Rotation Due to MgADP. The orientations of the LC domains can be determined from spectra of oriented samples, shown in Figure 2 (previously discussed in refs *23* and *26*). Labeled gizzard muscle sections were aligned with their filament axis parallel (Figure 2B) or perpendicular to the applied magnetic field. There are three spectral components, labeled P1−P3 in the low- and high-field regions; their central peaks overlap to form the prominent central peak. Upon addition of MgADP, the intensity in P1 increases, while that in P2 decreases. The change is small, but was observed consistently in all experiments ($n > 20$). The intensity of P3 was unchanged by addition of MgADP; the apparent change in Figure 2B is due to overlap with P2.

Each spectral component arises from a distinct population of spin probes. P3 (Figure 2B) appears to be very similar in these oriented samples to M2 in the isotropic samples (Figure 2A), and is largely insensitive to sample orientation or solution conditions. We therefore identify it with M2, and conclude that it contains no useable information about protein orientation. Thus, P1 and P2 arise from M1, and represent two distinct orientations of the LC domain.

The difference between P1 and P2 was modeled as a change in the axial tilt angle θ between the probe and filament axis. We assumed a distribution of probes in each population, with a full width at half-maximum $\Delta\theta$. A grid search-type algorithm was used to identify the best-fit θ and $\Delta\theta$ of each spectral component, comparing them to spectra simulated from a solution to the spin Hamiltonian using a program written by P. Fajer (*38*). The mobility of the probe reduces its anisotropy, so the difference between the best-fit central angles represents a lower limit on the actual difference. The best-fit simulated spectra for P1 and P2 were very similar to those for their counterparts in spectra of S1 (*23*). P1 was fit well with a θ_0 of 48 ± 3° and a $\Delta\theta$ of 16 ± 4°; this is the orientation adopted by the LC domain of smooth muscle S1 in the presence of MgADP, and by the LC domain of skeletal muscle myosin with or without MgADP. P2 corresponded to a θ_0 of 72 ± 3° and a $\Delta\theta$ of 16 ± 4°; this is the major orientation adopted by smooth muscle S1 LC domains in the absence of MgADP.

Thus, there are two populations of oriented probes in smooth muscle sections, distinguished by a ∼24° axial rotation. Fits to these spectra (Figure 2) and those for S1 (*23*) were very similar, allowing us to identify P1 and P2 as being equivalent to their counterparts in S1. We conclude that the LC domain of smooth muscle myosin can adopt either the intermediate or the final orientation, described above. The increase in P1 intensity and decrease in P2 intensity upon addition of MgADP (Figure 2B) indicates a net flux of probes, and hence LC domains, from one state to the other; i.e., a ∼24° axial rotation of LC domains from the final position, which gives rise to P2, to the intermediate position, which gives rise to P1.

The process of determining the best fits revealed a systematic error in our previous work; these results therefore constitute a minor correction, about 10°, to the absolute orientations published previously (*23*, *26*). An additional correction is that, on the basis of these fits, the population of smooth S1 LC domains in the intermediate state in the absence of MgADP was 20 ± 5%, similar to but slightly more than the value of ∼16% previously published (*23*).

We consider the relative intensities of P1 and P2 to be representative of all cross bridges in the muscle section. P1 and P2 changed in a coordinated fashion upon addition of MgADP, while P3 was insensitive to solution conditions. While it is possible that P3 represents cross bridges not bound to actin or otherwise behaving unlike those giving rise to P1 and P2, we consider this to be unlikely for two reasons. First, P3 was also present and behaved similarly in studies of S1, in which all heads were bound to actin and presumably experienced identical steric constraints (*23*). Second, the high levels (∼90%) of RLC exchange in some preparations (see Materials and Methods), and the uniformity of results across preparations, make it highly unlikely that we preferentially labeled any subset of cross bridges. Rather, the variability in P3 and M2 can be at least partially explained by observing that nonspecifically bound RLCs would be expected to give rise to a random, poorly immobilized spectrum. Indeed, the P3 population in muscle fibers was generally somewhat higher than previously observed in spectra of labeled S1 (*23*), in which little contribution from nonspecifically bound light chains is expected. We conclude that P3 represented both probes that were mobile and/or disordered, but bound to LC domains that behaved in a manner identical to that of those underlying P1 and P2 (in analogy to spectra of S1), and/or probes on RLCs that were not properly bound to LC domains.

How Many LC Domains Rotate? To measure the relative intensities of P1 and P2, spectra of labeled muscle sections in the presence and absence of MgADP were compared to the corresponding spectra of S1, in which relative intensities were known with fair accuracy (see Table 1). The spectra were fit in the low-field region to a linear combination of the S1 spectra by the method of least-squares (see Figure 3A). A good fit could not be obtained for all preparations, since P3 varies in intensity between preparations, and to a small degree qualitatively between S1 and intact muscle. In the absence of MgADP, 52 ± 8% (mean ± standard deviation) of the total P1 and P2 intensity was in P1 in dephosphorylated samples; in the presence of saturating MgADP, the value was 69 ± 5% (nine samples fit). Results were similar for thiophosphorylated preparations: 51 ± 8% in the absence of MgADP and 67 ± 6% in the presence of saturating MgADP (four samples fit). Hence, in the absence of MgADP the two LC domain conformations are equally populated. Upon addition of saturating MgADP, only about one-third of the LC domains remain in the final position, indicating a net rotation of ∼17% of LC domains from the final position to the intermediate position. These results are

Table 1: Axial Rotation of LC Domains

	apparent K_d (μM) (MgADP)	fraction of heads in the intermediate state (%) without MgADP	with MgADP[a]
skeletal S1[b]	–	100	100
smooth S1[b]	4.4 ± 2.5[c]	20 ± 5[b,d]	100 ± 5[b,d]
thiophosphorylated	6 ± 3[c]	22 ± 10[d]	97 ± 10[d]
smooth muscle	110 ± 20[c]	52 ± 3[d]	69 ± 2[d]
thiophosphorylated	730 ± 100[c]	53 ± 5[d]	67 ± 4[d]

[a] Saturating MgADP: 3.5 mM for dephosphorylated samples and 16.6 mM for thiophosphorylated samples. [b] Data reanalyzed from previous work (*23*). Uncertainty in the intermediate state population reflects the fitting method described therein. [c] Binding curves fit by the method of nonlinear least squares; errors represent asymptotic 95% confidence levels. [d] Values are the mean ± standard error of the mean, except for dephosphorylated S1 as noted. The number of experiments was as follows: three with dephosphorylated smooth S1, two with thiophosphorylated smooth S1, nine with dephosphorylated muscle, and four with thiophosphorylated muscle.

summarized in Table 1. The spectral change could be reversed by extensive washing of the sample with a nucleotide-free buffer containing excess EDTA, or by treatment with apyrase or myokinase to degrade nucleotides to AMP, returning the population of P1 to about 50%.

Dependence of the Rotation on MgADP Concentration. The MgADP concentration dependence of the LC domain rotation was determined by monitoring the extent of spectral change while titrating ADP into labeled muscle sections. The spectra at each MgADP concentration were fit by the method of least squares to a linear combination of the spectra recorded in the absence of ADP (sections washed for 2−4 h in 10 mM EDTA to remove all nucleotide) and in the presence of saturating MgADP (see Materials and Methods). Titrations are plotted in Figure 3 as a fraction of the full effect at saturating MgADP versus MgADP concentration. This range corresponds to a change in the intermediate state population from about 50% of the total LC domains without MgADP to about 68% at saturating MgADP (see the right-hand abscissa of Figure 3B). The data were fit by the method of least squares to a simple, noncooperative binding curve, of the form

$$\text{fraction of full effect} = [\text{MgADP}]/([\text{MgADP}] + K)$$

where $K = 110 \pm 20$ μM for dephosphorylated muscle sections. K here is an apparent dissociation constant, not necessarily equal to the actual K_d for MgADP binding to myosin (see the Discussion).

Thiophosphorylation of the RLC had a significant effect on this relationship. Muscle sections were labeled and thiophosphorylated as described in Materials and Methods, and the level of thiophosphorylation was determined by gel electrophoresis. Dephosphorylated samples, described above, had basal phosphorylation levels of 0−10%. Complete (90−100%) thiophosphorylation had no effect on the spectra recorded in the absence of MgADP or with saturating MgADP, as described above (summarized in Table 1), and hence no effect on LC domain orientation or mobility. However, as shown in Figure 3, the MgADP concentration required to effect rotation increased 7-fold, to half-effect at 730 ± 100 μM. In contrast, thiophosphorylation of labeled

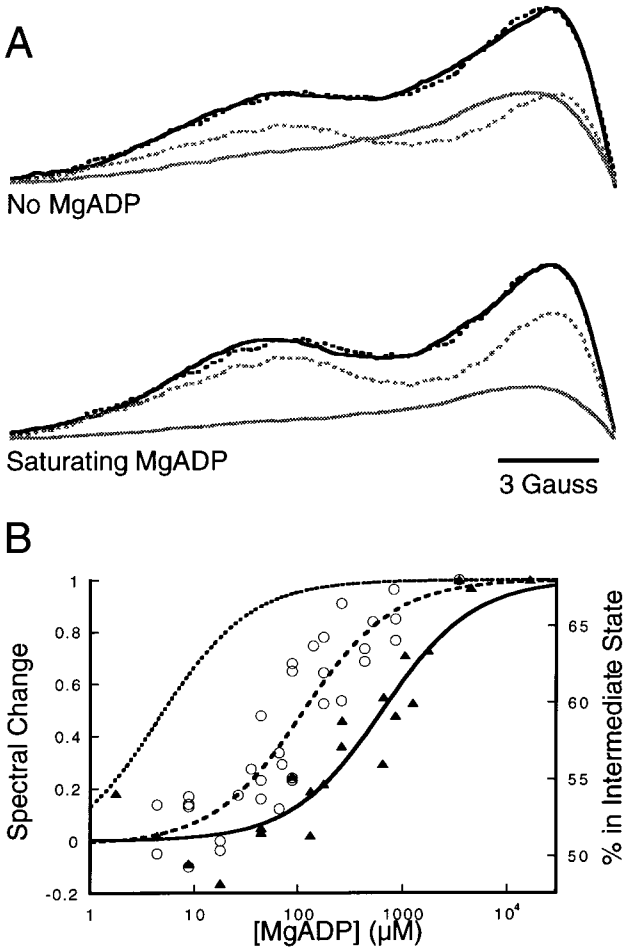

FIGURE 3: (A) Deconvolution of gizzard muscle spectra using S1 spectra. The low-field portions of representative spectra of muscle sections, aligned parallel to the magnetic field, (top) in the absence of MgADP and (bottom) in the presence of 3.5 mM MgADP, are shown (solid, black lines). Both spectra are fit well by linear combinations (dashed, black lines) of the spectra of labeled gizzard S1, bound to psoas fibers aligned parallel to the magnetic field, in the absence of MgADP (solid, gray lines) and in the presence of saturating (3.5 mM) MgADP (dashed, gray lines). The S1 spectra are shown in the best-fit proportions; the top spectrum (no MgADP) is fit by roughly equal intensities of the two S1 spectra, whereas the bottom spectrum (saturating MgADP) is fit by a preponderance of the S1 + MgADP spectrum, and a smaller contribution from the S1 − MgADP spectrum. (B) Extent of spectral change vs MgADP concentration: (○, − − −) dephosphorylated gizzard sections (six titrations), (▲, —) thiophosphorylated gizzard sections (four titrations), and (- - -) equivalent curve for gizzard S1 in psoas fibers (*23*). The spectrum of each sample at each MgADP concentration was fit to a linear combination of the spectra of that sample with no MgADP and with saturating MgADP (3.5 mM for dephosphorylated muscle and 16.6 mM for thiophosphorylated muscle). Each data set was fit individually to a simple binding curve (see the text) and normalized. Data sets from like samples were then combined and refit to produce the curves that are shown. The apparent $K_d = 4.4 \pm 2.5$ μM for S1, 110 ± 20 μM for dephosphorylated smooth muscle, and 730 ± 100 μM for thiophosphorylated smooth muscle. The right-hand axis indicates the population of LC domains in the intermediate state, assuming ~50% in the absence of MgADP and ~68% in saturating MgADP (see the text).

smooth S1 did not alter the LC domain orientation, distribution, or apparent MgADP affinity (data not shown) as compared to our previous experiments with dephosphorylated smooth S1 (*23*). Thus, thiophosphorylation of the RLC greatly increased the MgADP concentration that was neces-

sary to cause rotation of the LC domain of smooth muscle myosin, but not S1.

Various controls were performed to establish that the observed spectral effect was a result of MgADP binding to myosin. Addition of 5 mM ATP to the rigor buffer, relaxing the muscle section, produced EPR spectra very similar to the spectra of isotropically disordered preparations (Figure 2A). Addition of 2 mM pyrophosphate or 5 mM AMP-PNP, an ATP analogue, to the rigor buffer had no effect on the rigor spectrum, suggesting that heads were neither rotated nor detached from actin in significant numbers. Dissociation from actin would not be expected under these conditions. Varying the ionic strength of the buffer with or without ADP had no effect ([KCl] = 0−200 mM). Varying the Mg^{2+} content from 0 (i.e., 10 mM EDTA) to 50 mM at constant ionic strength, with or without ADP, also had no effect. Addition of 1 mM pyrophosphate inhibited the effect of MgADP, reducing the effect of adding (to a dephosphorylated sample) 100 μM ADP by about 50%, strongly suggesting that ADP binding at the nucleotide binding site of myosin produced the observed spectral change.

Nucleotide State of Myosin Heads. In gizzard sections in the absence of MgADP, ~50% of the cross bridges were found in the intermediate state. However, for S1 in the absence of MgADP the final conformation is predominant (~80%) (*23*). This raised the possibility that some heads retained MgADP despite efforts to remove all nucleotide prior to the experiment. To determine whether MgADP was still bound to myosin heads in our putatively ADP-free samples, binding of ϵADP, a fluorescent ADP analogue, was monitored via fluorescence spectroscopy. Mg·ϵADP was observed to produce a rotation identical to that produced by MgADP, except that a higher concentration was required (apparent K_d of ≈400 μM for Mg·ϵADP in dephosphorylated muscle), presumably due to a reduced affinity for the myosin head. Muscle sections were placed at the focus of an epifluorescence microscope and relaxed with ϵATP in the presence of 400 mM acrylamide, an agent that selectively quenches free ϵATP. The relaxing solution was then replaced with rigor solution containing 400 mM acrylamide, and the section was washed while fluorescence levels were recorded. Similar experiments using EPR, as described above, showed that washing returned the intermediate state population to ~50%. However, fluorescence declined to within 5% of maximal fluorescence above baseline with a half-life of several minutes (data not shown), indicating that no more than 5% of heads, if any, retained bound ϵADP after washing.

Time Dependence of the Spectral Effect. ADPase or other ADP-degrading activity in the skinned muscle sections could prevent accurate measurement of the MgADP concentration dependence of rotation. To assay the effect of any such activity on our measurements, labeled muscle sections were incubated in 110 μM MgADP and spectra were recorded over the course of 100 min with no further addition of ADP. The intermediate state population was maximally sensitive to MgADP concentration at this concentration (see Figure 3). Spectra were then fit to spectra recorded with no and 3.5 mM MgADP, as described above. Only a very small decline (0−10%) in the intermediate state population was seen after 100 min. Data for other experiments were typically collected for ≤20 min at each MgADP concentration, averaging to reduce noise. Hence, the apparent MgADP concentration was slightly overestimated due to degradation of ADP during data collection; however, the effect was not large, and no corrections have been applied to the data.

Effect of Tension on Spectra. An external tension or stretch applied to muscle fibers in rigor might cause the LC domains to rotate "backward", i.e., from the final state to the intermediate state. To investigate this possibility, we applied a constant tension to muscle sections, by attaching a small weight to one end of the section, while recording EPR spectra. At all tensions up to sufficient force to break the muscle section (0.4−0.5 N/mm^2), tension had no discernible effect on the spectra of muscle sections either in the absence of ADP or in the presence of 35−110 μM MgADP, where the spectra might be thought to be most sensitive to small changes in the stability of one state versus the other (data not shown). This observation is a corollary to the observation that MgADP binding does not reduce tension in smooth muscle sections (*39*).

DISCUSSION

We draw four conclusions from the results presented above, which are summarized in Table 1. These are discussed below, with emphasis on the comparison between the current results, obtained with smooth muscle sections, and previous results obtained with skeletal and smooth S1 (*23*, *26*).

The LC Domain of Smooth Muscle Rotates upon MgADP Release. The axial rotation of the LC domain seen in smooth muscle S1 upon ADP release also occurs in intact myosin in skinned muscle. Starting from the intermediate position (that of S1 with ADP bound), some LC domains (see below) rotate upon ADP release ~24° axially toward the barbed end of the actin filament, or away from the center of the myosin filament, to the final position (*21*). Both smooth muscle myosin and S1 are thus capable, upon ADP release, of an "extra" rotation in the direction of the putative power stroke that is not observed in skeletal muscle (*23*).

The intermediate and final states characterized here for smooth muscle myosin are very similar to those adopted by smooth muscle S1 (*23*). Under the experimental conditions employed here, it is likely that the two heads of each myosin are bound to adjacent actin monomers. The fact that only the intermediate and final states were observed suggests that it is reasonable to assume that the S1 structures described by Whittaker et al. (*21*) closely match the structures of the two heads of a single myosin under these conditions. EPR and other spectroscopic studies of skeletal muscle myosin and S1 likewise show that myosin heads and S1 bound to actin adopt very similar conformations (*26*, *40*, *41*); this entails a single orientation of the LC domain similar to the intermediate state of smooth muscle S1 (*23*), rather than the two orientations described here for smooth muscle myosin and S1. EM micrographs of isolated myosin molecules show that the two heads converge at the head−rod junction, such that the RLCs are in close proximity (*42*, *43*), but our spectra suggest that this is not the preferred conformation when both heads are bound to actin. Using the Whittaker et al. (*21*) structures as a guide, and allowing each head to adopt either the intermediate or final state, we find the closest possible approach of equivalent points at the distal (from actin) tips of the two RLCs of smooth muscle myosin to be ~80 Å. To allow for this head separation, the region of the coiled-

coil S2 domain proximal to the heads must uncoil. The proximal portion of this domain is unstable (*44*, *45*), and such uncoiling has been observed (*46*, *47*). This uncoiling will undoubtedly apply a restoring force to the heads, tending to pull them back together. This feature of the system is critical to the model we present (see below) to account for the measured populations of the intermediate and final states.

There Is a Relatively Small Change in the Populations of the Intermediate and Final States upon MgADP Release from Muscle As Compared to S1. The EPR method used here can report not only on the magnitude of the differences in LC domain orientation but also on the relative populations of each state present in a mixture. Our previous study with smooth S1 gave relatively large differences between spectra under extreme MgADP concentration conditions. In the absence of ADP, ~80% of the LC domains were in the final conformation, with ~20% in the intermediate conformation. In the presence of saturating MgADP, 100% of the LC domains were in the intermediate conformation (*23*). In contrast to the S1 spectra, the corresponding data for intact myosin in muscle sections exhibited a relatively small difference between spectra under extreme MgADP concentration conditions (Figure 2B and Table 1). In the absence of MgADP, the LC domains of intact myosin were distributed more or less evenly across the intermediate and final states (~52% in the intermediate state). Upon addition of saturating MgADP, about one-sixth of the LC domains (net) rotated from the final position to the intermediate position (~69% in the intermediate state, total).

We performed two experiments to demonstrate that the relatively high proportion (~52%) of LC domains in the intermediate state in intact myosin with MgADP removed was not due to residual MgADP binding at the active site. First, the fraction of heads in the intermediate state could not be reduced by treatment with either apyrase or myokinase, enzymes that degrade ADP, or by extensive washing with 10 mM EDTA to chelate free Mg^{2+} and thus eliminate rebinding of released ADP. Second, because the fluorescent nucleotide analogue ϵADP caused the same EPR spectral change as ADP, we used fluorescence intensity to monitor the residual ϵADP concentration during washing protocols used in EPR experiments; ≤5% of the heads remained bound to ϵADP after washing following relaxation with ϵATP.

Our population measurements do to some degree depend on the efficiency of RLC labeling, and in particular upon any bias in labeling different populations of heads. As noted in Materials and Methods, the efficiency of exchange of labeled for unlabeled RLC reached as high as 90% in some preparations, rendering it unlikely that preferential labeling of a particular population of heads skewed our measurements. Excessive amounts of nonspecifically bound, labeled RLC, which contributes to the mobile P3 population, could also skew these numbers by introducing a high "background" signal. We therefore restricted analysis to preparations that could be deconvoluted using spectra of labeled S1, as described above, which eliminated contributions from preparations with a high P3 intensity.

Muscle Has a Different MgADP Concentration Dependence of Rotation Compared to S1. We used the spectral change caused by LC domain rotation to compare the ability of MgADP to affect the distribution between the intermediate and final states in different preparations: S1 versus muscle and dephosphorylated versus thiophosphorylated. Previously, we had found that the apparent K_d for the transition in dephosphorylated smooth S1 was ~4.4 μM MgADP (*23*). Here we find that the apparent K_d for dephosphorylated muscle sections is ~110 μM MgADP, suggesting a greater energetic barrier to rotation.

The interpretation of these apparent K_d values must be carefully considered. The data fit well to a simple binding isotherm (Figure 3), suggesting that the rotation of an individual LC domain is directly related to MgADP binding. However, we cannot overemphasize the fact that these experiments do not report on MgADP binding, but rather only on the spectral changes induced by MgADP. Thus, these experiments do not measure the affinity of the heads for MgADP. The actual affinities for MgADP may be different for the two heads of a single myosin and/or dependent on steric constraints, in that some heads may be binding to MgADP without causing a rotation of the LC domain (see below).

Thiophosphorylation Alters the MgADP Concentration Dependence of Rotation in Muscle. Upon thiophosphorylation of Ser-19 of the RLC, significantly more MgADP was required to produce the observed rotation; the apparent K_d was ~730 μM MgADP, about 7 times greater than the K_d measured in dephosphorylated preparations. However, the distribution of heads between the intermediate state and final state was not altered under the extreme conditions of no, or saturating, MgADP. Thiophosphorylation does not appear to alter the states that can be accessed by myosin, but does weaken the ability of MgADP to affect the distribution between the states. This ~7-fold decrease in the apparent affinity for MgADP due to thiophosphorylation is similar to the 3.5-fold decrease in the apparent affinity of rigor cross bridges for ADP upon thiophosphorylation measured previously in α-toxin-permeabilized smooth muscle, although the absolute magnitudes of the constants are different (*15*).

A Simple Model. The differences listed above between myosin in skinned muscle on one hand, and S1 on the other, summarized in Table 1, can be explained with a simple model involving steric constraints between the two heads of a myosin molecule bound to actin (Figure 4). Since our data show loose coupling between the nucleotide state and conformational state, we assume any myosin head strongly bound to actin may adopt one of four states: intermediate, no nucleotide ($A{\cdot}M_I$); intermediate, MgADP bound ($A{\cdot}M_I{\cdot}D$); final, no nucleotide ($A{\cdot}M_F$); or final, MgADP bound ($A{\cdot}M_F{\cdot}D$) (defined in the legend of Figure 4). Our data reflect the ratio of the total occupancy of the intermediate states ($A{\cdot}M_I$ and $A{\cdot}M_I{\cdot}D$) to the total occupancy of the final states ($A{\cdot}M_F$ and $A{\cdot}M_F{\cdot}D$).

From the spectral response to MgADP in both smooth S1 and muscle preparations, we derive the first major element of our model.

(1) MgADP binding in the active site of smooth muscle myosin influences the orientation of the LC domain, favoring the intermediate state.

Upon MgADP binding or release, conformational changes in the active site presumably cause internal strains in the head, which influence the LC domain orientation. In the case of S1 (Figures 4 and 5, right side), MgADP binding induces LC domain reorientation. In the absence of MgADP, there

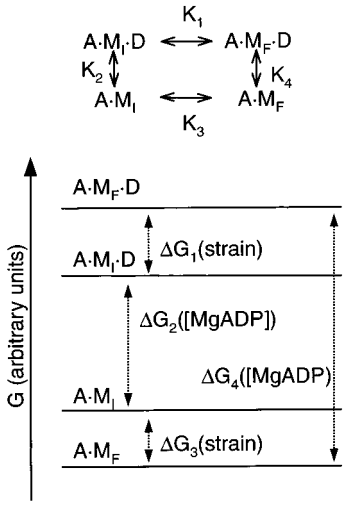

FIGURE 4: Simple thermodynamic model. Energy levels presented are qualitatively correct for S1 with $0 < [\text{MgADP}] \ll K_d$ (e.g., 1 μM MgADP). ΔG_1 corresponds to K_1, etc. A strongly bound myosin head can occupy one of the four states depicted, where A is actin, M_I is myosin in the intermediate state, M_F is myosin in the final state, and D is MgADP. The stability of the ADP-bound states relative to the corresponding no-nucleotide states (ΔG_2 and ΔG_4) is a function of MgADP concentration. The relative stability of the two conformational states in the same nucleotide state (ΔG_1 and ΔG_3) is a function of the total strains, internal and external, on the head. Thus, in the case that is depicted, the $A{\cdot}M_F$ state is most stable and preferentially populated, although a significant population of heads are in the $A{\cdot}M_I$ state. A MgADP concentration much greater than K_d would greatly stabilize the ADP-bound states (moving them below the nucleotide-free states in the diagram), so $A{\cdot}M_I{\cdot}D$ would be most favored. Negative strain, as experienced by trailing heads (see Figure 5), would stabilize (lower) the final states relative to the intermediate states, so that in the presence of high MgADP concentrations the $A{\cdot}M_F{\cdot}D$ state would be favored over $A{\cdot}M_I{\cdot}D$.

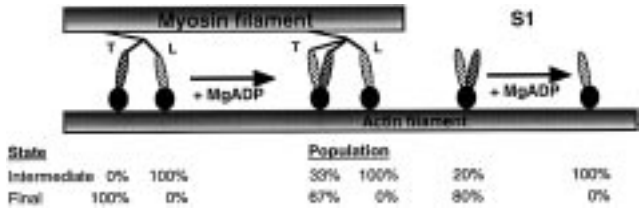

FIGURE 5: Cartoon illustrating the constraints on LC domain orientation in muscle. S1 is presented on the right, for comparison. Catalytic domains are drawn as shaded circles and LC domains as ovals. The two heads of a single myosin bind to adjacent actin monomers. The two LC domains are connected by their heavy chains to a coiled coil, which in turn connects them to the thick filament. Part of the coiled coil is pulled apart to allow both heads to bind. The fraction of leading heads (right head of each pair, labeled L) or trailing heads (left heads, labeled T) in each of the intermediate and final states is denoted below the head in question. Total populations of either state are taken from experimental data (Table 1); assignment to the leading or trailing head is based on the model presented here, and given as the fraction of that head in either state. In the absence of MgADP, the leading head's LC domain is pulled back into the intermediate conformation, whereas the trailing LC domain is pulled forward into the final conformation. With MgADP present, the leading LC domain is still pulled back into the intermediate conformation, but upon binding of MgADP, a fraction of the trailing LC domains are able to rotate back into the intermediate conformation as well.

is a mixture of states, with ~80% of the LC domains in the final ($A{\cdot}M_F$) state. This indicates that with no nucleotide bound, the final ($A{\cdot}M_F$) state is more stable than the intermediate ($A{\cdot}M_I$) state by about 1.4 kT ($=\Delta G_3$). However, in the presence of saturating MgADP, all LC domains adopt the intermediate conformation (*23*), indicating that with MgADP bound the intermediate ($A{\cdot}M_I{\cdot}D$) state is significantly more stable than the final ($A{\cdot}M_F{\cdot}D$) state ($\Delta G_1 \geq$ 2.3 kT, on the assumption that our experimental technique would detect a population of 10% in the final state).

Intact myosin in muscle sections (Figure 5, left side) differs, in that the population distributions are more nearly equal and the net change in distribution is much smaller upon addition of MgADP. The coupling between the nucleotide state and LC domain orientation is more complex than in S1, showing that additional constraints not felt by S1 influence the LC domain orientation. This observation leads to the second major element of our model.

(2) LC domain orientation is influenced by steric constraints on the myosin head.

The most obvious difference between S1 and the intact myosin in our muscle sections is in the external constraints and forces on the myosin heads. S1 is free of all external constraints except the actomyosin bond. In contrast, as discussed above, strong binding of both myosin heads to actin requires uncoiling of the coiled-coil domain. This provides a restoring force on the LC domains, pulling them back together and resisting further separation. As illustrated in Figure 5, the geometry of the two head−actin complex suggests that the trailing head of a pair is pulled forward, biasing it to the final state [stabilizing $A{\cdot}M_F$ relative to $A{\cdot}M_I$ by some amount, and $A{\cdot}M_F{\cdot}D$ relative to $A{\cdot}M_I{\cdot}D$ by about 0.7 kT according to our model (see Figure 5)], while the leading head is pulled backward, biasing it to the intermediate state (stabilizing $A{\cdot}M_I$ relative to $A{\cdot}M_F$, and $A{\cdot}M_I{\cdot}D$ relative to $A{\cdot}M_F{\cdot}D$). Any other conformation of the two heads (e.g., both LC domains in the intermediate position) requires a greater separation and presumably further stretching or uncoiling of the connection between the two heads, and is therefore energetically less favorable. A similar geometric model has recently been proposed to explain observations of skeletal HMM actin binding kinetics (*48*). Additionally, strain can be imposed by the connection of the two heads to the myosin filament. As discussed below, this is generally a backward force on the leading head, with less effect on the trailing head.

On the basis of our data on population distributions (Table 1), we consider it likely that forces external to the myosin heads are sufficient in the absence of MgADP to cause trailing heads overwhelmingly to adopt the final conformation ($A{\cdot}M_F$) and leading heads overwhelmingly to adopt the intermediate conformation ($A{\cdot}M_I$), as shown in Figure 5. This would produce the equal distribution between states in the absence of MgADP seen in our data. Upon MgADP binding to leading heads, no rotation of LC domains occurs, since the leading heads are already in the conformation favored by MgADP binding and merely go from the $A{\cdot}M_I$ state to $A{\cdot}M_I{\cdot}D$. This model predicts that the affinity of leading heads for MgADP is enhanced by the steric stabilization of the intermediate state. MgADP binding to trailing heads produces a different result (Figure 5). The trailing heads occupy the final ($A{\cdot}M_F$) state, and can rotate to the intermediate state upon MgADP binding. However, the internal strains favoring rotation upon MgADP binding are counteracted by the external strains opposing it. Our data

suggest that the equilibrium of forces results in about one-third of the trailing heads adopting the intermediate ($A{\cdot}M_I{\cdot}D$) state in the presence of saturating MgADP, while the rest adopt the final ($A{\cdot}M_F{\cdot}D$) state. In this model, this interplay of forces reduces the true affinity of trailing heads for MgADP.

This model predicts that a higher MgADP concentration is required to rotate myosin LC domains, as compared to S1 LC domains, as seen in our data. In rotating from the final position to the intermediate position, the trailing head moves farther from the leading head by several angstroms, doing work against the restoring force imposed by the connecting protein (Figure 5, compare the left side vs the right side). The ~25-fold difference observed in the apparent K_d in the case of dephosphorylated heads implies an energetic cost of ~3 kT for separating the heads by this distance.

The model also predicts the result that externally applied tension, stretching the fiber, should have little effect on the distribution of heads between the intermediate and final states in rigor fibers, as observed. A stretch would tend to drive cross bridges backward along their cycle, the opposite of normal contraction. However, most of the backward strain is taken up by the leading head of any pair, which is already in the intermediate position (see Figure 5). The trailing head would experience little, if any, strain until the leading head was forcibly dissociated from actin. Equally, MgADP binding would alter the conformation only of the trailing, less strained head. The actual change in muscle tension upon MgADP binding would depend on the details of the connection between the heads and the distribution of strain between them, but would be predicted to be small, as observed by Dantzig et al. (*39*) who saw a very slight increase in tension upon MgADP binding in gizzard muscle.

By its nature, this model suggests that the apparent K_d for MgADP (110 μM) measured in our experiments is not the true dissociation constant for dissociation of MgADP from actomyosin. If stabilization of the intermediate state equates to stabilization of MgADP binding (see the discussion of latch, below), then the leading and trailing heads would be expected to have different affinities for MgADP. Moreover, in our experiments, we observe only the total populations of the intermediate and final states ($[A{\cdot}M_I] + [A{\cdot}M_I{\cdot}D]$ vs $[A{\cdot}M_F] + [A{\cdot}M_F{\cdot}D]$), without reference to nucleotide state. Thus, the quantity plotted in Figure 3 is ($[A{\cdot}M_I] + [A{\cdot}M_I{\cdot}D]$)/[all heads], whereas the true measure of heads with MgADP bound is ($[A{\cdot}M_I{\cdot}D] + [A{\cdot}M_F{\cdot}D]$)/[all heads]. Increasing the MgADP concentration causes these quantities to change at different rates, producing a difference between our apparent K_d and the true value.

Latch. The influence of MgADP concentration, strain, and extent of RLC phosphorylation on LC domain orientation in our experiments and model suggest, tantalizingly, that the observed LC domain rotation may be important to the latch state of smooth muscle. Although there is little direct evidence, it is considered likely that in an active fiber, only one head of a given myosin interacts with actin at any given time (the situation in Figure 6). Our results and the model presented above, arising from a nonphysiological "rigor" system with both heads strongly bound to actin, must be applied to active muscle only very cautiously. Nevertheless, a conservative extension of our model provides a workable model for the behavior of latch bridges in the late stages of smooth muscle contraction.

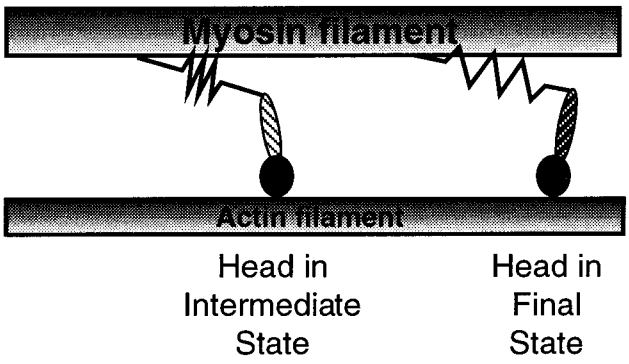

FIGURE 6: Cartoon illustrating the energetics of LC domain rotation in active, isometric muscle. We assume only one head of a given myosin will interact with actin at a time. The head is connected to the rod via a compliant element. The compliant element could be in S2, as depicted here, or it could be in the LC domain itself. If the cross bridge is under strain, rotating from the intermediate state to the final state necessitates pulling out the compliant element, at an energetic cost. The intermediate state is therefore stabilized by strain on the cross bridge.

The first additional element of the model is as follows.

(3) A smooth myosin head in the final ($A{\cdot}M_F$) state can detach rapidly from actin, but detachment is much slower from the intermediate ($A{\cdot}M_I$ or $A{\cdot}M_I{\cdot}D$) state.

Several factors could satisfy this requirement; ADP release, ATP binding, and/or release of the myosin head from actin could be much less favorable in the intermediate state than in the final state. Any one could equate to a virtual requirement for LC domain rotation to the final position before the completion of one ATPase cycle and the start of another. We have argued above that backward strain, as experienced by leading heads in our model (or, equally, resistance to shortening, as experienced by working heads under the near-isometric conditions of latch), stabilizes the intermediate state, as illustrated in Figure 6. Thus, a head under backward strain, like a leading head in our model, would have enhanced affinity for MgADP, whereas a head under forward strain, like a trailing head, would have decreased MgADP affinity. It is an easy leap from these thermodynamic statements to a kinetic argument: strain-dependent stabilization of the intermediate state slows the ATPase cycle, possibly by delaying ADP release as suggested by Barsotti et al. (*49*) and by Cremo and Geeves (*32*). A strain dependence of product release was also proposed by A. F. Huxley in the first model of muscle contraction (*50*), where product release and MgATP binding occur much more slowly in cross bridges that are exerting positive force. Our data in fact suggest that MgADP release from the intermediate ($A{\cdot}M_I{\cdot}D$) state could be slow, since in S1 the $A{\cdot}M_I{\cdot}D$ state is more stable than the $A{\cdot}M_I$ state (Table 1). A strain-dependent molecular mechanism of this sort could account for the Fenn effect, in that a muscle under tension would consume less ATP and produce less heat than would a freely contracting muscle (*51*).

MgADP concentration is another factor affecting the rate of actomyosin ATPase. MgADP competes with MgATP for binding the myosin head so that detachment of the head from actin is increasingly delayed by higher concentrations of MgADP (*15*). Our results show that, if point 3 of our model

is correct, MgADP binding has an additional, more subtle effect. It biases the head to the intermediate ($A{\cdot}M_I{\cdot}D$) state, further delaying detachment by reducing the fraction of time the head spends in the final ($A{\cdot}M_F$ or $A{\cdot}M_F{\cdot}D$) state. An elevated MgADP concentration associated with contraction has been observed in intact preparations of tonic smooth muscle (*52*), which exhibits a pronounced latch state, but not in phasic smooth muscle (*53*), in which latch is markedly less distinct. The MgADP concentration has been observed to rise modestly over the course of permeabilized smooth muscle contraction (*54*), which would tend to enhance this effect late in contraction. The same work indicates that latch-like behavior is only observed in the presence of a sufficiently high [MgADP]/[MgATP] ratio. Tellingly, MgADP affinity is higher in tonic smooth muscle than in phasic muscle (*13*, *17*). We note, also, that a strongly bound head under no particular strain is likely to act like S1, in that its state is a function primarily of whether MgADP is bound, until MgATP successfully detaches it from actin.

The first three elements of our model have the potential to explain the behavior of slowly cycling latch bridges: strain on myosin heads and MgADP binding serve to delay detachment from actin, reducing energy consumption and prolonging occupancy of a post-power stroke, force-generating state of the myosin head, thus enhancing the economy of tension maintenance. What is missing from this picture is a switch, converting a rapidly contracting, active muscle into a slowly contracting, economical latch muscle. Any effect that changed the relative stabilities of the intermediate and final states, stabilizing the final state in the early stages of contraction and the intermediate state late in contraction, would serve to promote the economical behavior described above more in latch than in early contraction. Our results suggest a candidate for that factor, leading to the final element of our model.

(4) Dephosphorylation of the RLC triggers latch-like behavior in myosin heads by a positive feedback mechanism.

Our results show that RLC phosphorylation changes the MgADP concentration dependence of the distribution of heads between the intermediate and final states. Importantly, RLC thiophosphorylation does not change the states that are accessible to the myosin head as defined by LC domain orientation, nor does it change the distribution of states in zero or saturating MgADP (see Table 1); this implies that the steric constraints on the LC domain do not change greatly upon phosphorylation. Rather, RLC phosphorylation only reduces the power of MgADP to effect the rotation of a myosin head from the final to the intermediate state. This suggests that the actual affinity of the myosin head for ADP is altered by RLC phosphorylation. We note that our experimental values for the apparent K_d of MgADP are not necessarily relevant to a working muscle. Nevertheless, RLC phosphorylation can reasonably be proposed to reduce the apparent affinity for MgADP in working muscle as well. The apparent role of MgADP in stabilizing high-force, low-phosphorylation states of smooth muscle (*54*) supports this proposal. Then in the absence of significant strain, phosphorylated heads would be relatively insensitive to MgADP and would cycle quickly through the intermediate state. Dephosphorylated heads would be more sensitive to MgADP (7-fold more sensitive, if our data apply) and would thus cycle less rapidly. RLC dephosphorylation late in contraction might therefore trigger a positive feedback loop. Dephosphorylated heads would cycle less quickly, slowing overall contraction. As the velocity of contraction slowed, active heads would experience greater resistance to rotation, stabilizing the intermediate state and reducing their cycling rate. Slower cycling rates would further slow contraction, and so on.

ACKNOWLEDGMENT

We thank Patricia Ellison, Kathy Franks-Skiba, G. Ramaprian, My Nyong Vo, and Xiangdong Wu for technical assistance.

REFERENCES

1. Somlyo, A. P. (1993) *J. Muscle Res. Cell Motil. 14*, 557−563.
2. Górecka, A., Aksoy, M. O., and Hartshorne, D. J. (1976) *Biochem. Biophys. Res. Commun. 71*, 325−331.
3. Sellers, J. R., Chock, P. B., and Adelstein, R. S. (1983) *J. Biol. Chem. 258*, 14181−14188.
4. Sellers, J. R. (1985) *J. Biol. Chem. 260*, 15815−15819.
5. Sellers, J. R. (1991) *Curr. Opin. Cell Biol. 3*, 98−104.
6. Tan, J. L., Ravid, S., and Spudich, J. A. (1992) *Annu. Rev. Biochem. 81*, 721−759.
7. Trybus, K. M. (1991) *Curr. Opin. Cell Biol. 3*, 105−111.
8. Warrick, H. M., and Spudich, J. A. (1987) *Annu. Rev. Cell Biol. 3*, 379−421.
9. Stull, J. T., Bowman, B. F., Gallagher, P. J., Herring, B. P., Hsu, L. C., Kamm, K. E., Kubota, Y., Leachman, S. A., Sweeney, H. L., and Tansey, M. G. (1990) *Prog. Clin. Biol. Res. 327*, 107−126.
10. Dillon, P. F., Aksoy, M. O., Driska, S. P., and Murphy, R. A. (1981) *Science 211*, 495−497.
11. Murphy, R. A. (1994) *FASEB J. 8*, 311−318.
12. Wingard, C. J., Paul, R. J., and Murphy, R. A. (1994) *J. Physiol. 481*, 111−117.
13. Fuglsang, A., Khromov, A., Torok, K., Somlyo, A. V., and Somlyo, A. P. (1993) *J. Muscle Res. Cell Motil. 14*, 666−677.
14. Horiuti, K., Somlyo, A. V., Goldman, Y. E., and Somlyo, A. P. (1989) *J. Gen. Physiol. 94*, 769−781.
15. Nishiye, E., Somlyo, A. V., Torok, K., and Somlyo, A. P. (1993) *J. Physiol. 460*, 247−271.
16. Rembold, C., and Murphy, R. (1993) *J. Muscle Res. Cell Motil. 14*, 325−333.
17. Khromov, A., Somlyo, A. V., Trentham, D. R., Zimmerman, B., and Somlyo, A. P. (1995) *Biophys. J. 69*, 2611−2622.
18. Somlyo, A. V., Goldman, Y. E., Fujimori, T., Bond, M., Trentham, D. R., and Somlyo, A. P. (1988) *J. Gen. Physiol. 91*, 165−192.
19. Rayment, I., Rypniewski, W. R., Schmidt-Base, K., Smith, R., Tomchick, D. R., Benning, M. M., Winkelmann, D. A., Wesenberg, G., and Holden, H. M. (1993) *Science 261*, 50−57.
20. Cooke, R. (1997) *Physiol. Rev. 77*, 671−697.
21. Whittaker, M., Wilson-Kubalek, E. M., Smith, J. E., Faust, L., Milligan, R. A., and Sweeney, H. L. (1995) *Nature 378*, 748−751.
22. Jontes, J. D., Wilson-Kubalek, E. M., and Milligan, R. A. (1995) *Nature 378*, 751−753.
23. Gollub, J., Cremo, C. R., and Cooke, R. (1996) *Nat. Struct. Biol. 3*, 796−802.
24. Baker, J. E., Brust-Mascher, I., Ramachandran, S., LaConte, L. E., and Thomas, D. D. (1998) *Proc. Natl. Acad. Sci. U.S.A. 95*, 2944−2949.
25. Dominguez, R., Freyzon, Y., Trybus, K. M., and Cohen, C. (1998) *Cell 94*, 559−571.
26. Zhao, L., Gollub, J., and Cooke, R. (1996) *Biochemistry 35*, 10158−10165.
27. Barnett, V. A., Fajer, P., Polnaszek, C. F., and Thomas, D. D. (1986) *Biophys. J. 49*, 144−146.

28. Thomas, D. D., and Cooke, R. (1980) *Biophys. J. 32*, 891−906.
29. Thomas, D. D. (1987) *Annu. Rev. Physiol. 46*, 691−709.
30. Ikebe, M., and Hartshorne, D. J. (1985) *J. Biol. Chem. 260*, 13146−13153.
31. Facemyer, K. C., and Cremo, C. R. (1992) *Bioconjugate Chem. 3*, 408−413.
32. Cremo, C. R., and Geeves, M. A. (1998) *Biochemistry 37*, 1969−1978.
33. Cremo, C. R., Sellers, J. R., and Facemyer, K. C. (1995) *J. Biol. Chem. 270*, 2171−2175.
34. Morita, J.-I., Takashi, R., and Ikebe, M. (1991) *Biochemistry 30*, 9539−9545.
35. Trybus, K. M., and Chatman, T. A. (1993) *J. Biol. Chem. 268*, 4412−4419.
36. Crowder, M. S., and Cooke, R. (1987) *Biophys. J. 51*, 323−333.
37. Griffith, O. H., and Jost, P. C. (1976) in *Spin Labeling: Theory and Applications* (Berliner, L. J., Ed.) pp 454−519, Academic Press, New York.
38. Fajer, P. G., Bennett, R. L. H., Polnaszek, C. F., Fajer, E. A., and Thomas, D. D. (1990) *J. Magn. Reson. 88*, 111−125.
39. Dantzig, J. A., Barsotti, R. J., Manz, S. A., Sweeney, H. L., and Goldman, Y. E. (1997) *Biophys. J. 72*, A128.
40. Sabido-David, C., Ferguson, R. E., Brandmeier, B. D., Hopkins, S. C., Goldman, Y. E., Kendrick-Jones, J., Dale, R. E., Corrie, J. E. T., Trentham, D. R., and Irving, M. (1997) *Biophys. J. 72*, A52.
41. Hambly, B., Franks, K., and Cooke, R. (1991) *Biophys. J. 59*, 127−138.
42. Walker, M., Knight, P., and Trinick, J. (1985) *J. Mol. Biol. 184*, 535−542.
43. Flicker, P. F., Walliman, T., and Vibert, P. (1983) *J. Mol. Biol. 169*, 723−741.
44. Málnási-Csizmadia, A., Shimony, E., Hegyi, G., Szent-Györgyi, A. G., and Nyitray, L. (1998) *Biochem. Biophys. Res. Commun. 252*, 595−601.
45. Trybus, K., Freyzon, Y., Faust, L., and Sweeney, H. (1997) *Proc. Natl. Acad. Sci. U.S.A. 94*, 48−52.
46. King, L., Seidel, J. C., and Lehrer, S. S. (1995) *Biochemistry 34*, 6770−6774.
47. Zhang, Y. Y., Shao, Z. F., Somlyo, A. P., and Somlyo, A. V. (1997) *Biophys. J. 72*, 1308−1318.
48. Conibear, P. B., and Geeves, M. A. (1998) *Biophys. J. 75*, 926−937.
49. Barsotti, R. J., Dantzig, J. A., and Goldman, Y. E. (1996) *Nat. Struct. Biol. 3*, 737−739.
50. Huxley, A. F. (1957) *Prog. Biophys. Biophys. Chem. 7*, 255−318.
51. Fenn, W. O. (1923) *J. Physiol. 58*, 175−203.
52. Krisanda, J. M., and Paul, R. J. (1983) *Am. J. Physiol. 244*, C385−C390.
53. Hellstrand, P., and Paul, R. J. (1983) *Am. J. Physiol. 244*, C250−C258.
54. Khromov, A., Somlyo, A. V., and Somlyo, A. P. (1998) *Biophys. J. 75*, 1926−1934.

BI990267E